The 2010 IEEE/RSJ International Conference on
Intelligent Robots and Systems
October 18-22, 2010, Taipei, Taiwan

State Dependent Control of a Robotic Manipulator used for Nuclear Decommissioning Activities

C. James Taylor, Arun Chotai and David Robertson

Abstract— **This article considers pole assignment control of nonlinear dynamic systems described by State Dependent Parameter (SDP) models, with a particular focus on a Brokk 40 mobile robot and Hydro–Lek HLK–7W two–arm manipulator used for nuclear decommissioning tasks. The UK nuclear legacy comprises a number of facilities that are significantly contaminated by radioactivity and non–radiological toxins. Here, the use of remote and teleoperated robotic solutions provide an invaluable option for the safe retrieval and disposal of contaminated materials. Since the behaviour of hydraulically–driven manipulators is dominated by the nonlinear, lightly–damped dynamics of the actuators, existing systems can suffer from a relatively slow and imprecise control action. For this reason, the research utilises a non–minimal state variable feedback approach to control system design, in which the control gains are updated at each sampling instant.**

I. Introduction

The UK nuclear legacy stems in part from the dawn of the nuclear industry and presents scientists and engineers with a host of semi–intractable challenges [1]. This legacy comprises a number of facilities that are significantly contaminated by radioactivity and non–radiological toxins, are sometimes in a relatively poor state of repair and for which knowledge of their use can be incomplete. In areas of significant contamination, it is often necessary to resort to the use of remote and teleoperated mobile robots. These provide an invaluable option for the safe retrieval and disposal of contaminated materials in high–hazard legacy facilities, whilst safeguarding the environment and minimising radiation exposure to operators [2] [3] [4].

In the early stages of clean–up, expensive, bespoke machines were designed, built and commissioned. However, these have suffered from reliability problems and were rarely transferable to other challenges. More recently, off–the–shelf remote solutions are strived for but these suffer from a converse restriction: they offer the benefits of generic design but not the ease of control afforded by high–specification bespoke solutions. The research described in this article aims to alleviate this unsatisfactory situation by affording optimized, widely applicable control architectures that will be developed and tested on an off–the–shelf mobile robotic platform, with a particular focus on the coordinated control of its dual–arm manipulators. These potentially have many advantages over single–arm robots because they introduce additional flexibility to, for example, generic cutting operations, whilst not risking the enormous expense of bespoke robotic design.

C. James Taylor and David Robertson are with the Engineering Department, Lancaster University, UK c.taylor@lancaster.ac.uk

Arun Chotai is with the Lancaster Environment Centre, Lancaster University, UK a.chotai@lancaster.ac.uk

The research utilises a BROKK 40 decommissioning robot, consisting of a moving vehicle with a single manipulator (Fig. 1). The multi–arm system attached to the Brokk 40 is the Hydro–Lek HLK–7W, which takes the form of two seven-function manipulators, i.e. six rotary joints and a gripper. Such dual arm mobile robots now offer a powerful tool for various types of decommissioning activity. Unfortunately, devices initially developed for heavy lifting are not necessarily suitable for 'soft touch' duties such as picking up relatively fragile objects. Indeed, under automatic (rather than remote) control, the manipulator above can suffer from a relatively slow and imprecise control action because of limitations in existing linear feedback algorithms.

Since the behaviour of hydraulically–driven manipulators is dominated by the nonlinear, lightly–damped dynamics of the actuators, high performance depends on the introduction of some type of nonlinear control structure. Research into nonlinear control embraces approaches such as sliding mode [5], adaptive [6], quasi–linear parameter varying [7] and state dependent Riccati equation (SDRE) control, among others. SDRE methods utilise a direct parameterisation to transform the nonlinear system into a linear–like structure [8]. Using this model, it mimics the Linear Quadratic (LQ) regulator, but yields a state variable feedback algorithm with time varying coefficients. Unfortunately, while some theoretical advances have been made regarding the asymptotic stability of SDRE methods, the conditions obtained can be difficult to check and/or fulfill.

The idea of designing control systems that assign the closed–loop eigenvalues (poles) at, or at least near to, specified desirable locations is appealing to many control engineers. For linear systems, the most powerful general method of pole assignment is state variable feedback (SVF). It is well known that a linear SVF control law can arbitrarily assign the closed–loop poles, provided the linear system is controllable [9]. Many approaches have been proposed to extend this concept to nonlinear systems, including local linearization, exact linearization by feedback [10] and the use of nonlinear transformations [11].

The present article focuses on a recently developed approach to nonlinear pole assignment using State Dependent Parameter (SDP) models [12]. Here, the control parameters are functionally dependent on the measured state variables of the system, such as joint angle or velocity. The nonlinear system is first modelled using the quasi–linear SDP structure, in which the parameters vary as functions of the state variables [13]. Using an analogy with linear Non–Minimal State Space (NMSS) methods [14] [15], state variable feed-

Fig. 1. Brokk mobile robot and Hydro–Lek dual–arm manipulator.

back control is subsequently implemented directly from the measured input and output signals and their delayed values. Linear NMSS methods have been successfully applied to mobile construction robots, such as automated excavators [16] and vibro–lance systems [17].

However, initial research into nonlinear SDP–NMSS control necessarily *assumed* global controllability and used linear methods such as pole assignment or LQ design to update the control parameters at each sampling instant (cf. SDRE design). Although such control systems have already proven useful in control of hydraulically–driven manipulators [18], the expected design response (even stability) does not necessarily follow in the nonlinear case. By contrast, the present article discusses a new transformation method that does guarantee stability at the design stage, and appears ideal for the control of the Hydro–Lek manipulator.

II. Control Framework

Consider the following nth order SDP model,

$$y_k = -a_1\{\boldsymbol{\chi}_k\}\, y_{k-1} - a_2\{\boldsymbol{\chi}_k\}\, y_{k-2} - \ldots - a_n\{\boldsymbol{\chi}_k\}\, y_{k-n} + b\{\boldsymbol{\chi}_k\}\, u_{k-\tau} \quad (1)$$

Here y_k and u_k are the output and control input variables respectively, while $a_i\{\boldsymbol{\chi}_k\}$ $(i = 1 \cdots n)$ and $b\{\boldsymbol{\chi}_k\}$ are state dependent parameters. The latter are assumed to be functions of a non–minimal state vector $\boldsymbol{\chi}_k$. These states are typically derived from the delayed control input and output signals, but could also be functions of any other measured variables. Finally, τ is the pure time (transport) delay of the system where, for the purposes of discrete–time control system design, $\tau \geq 1$. For brevity, the SDP model parameters will henceforth be denoted with a subscript k, representing the sample number. Hence, (1) is equivalently,

$$y_k = -a_{1,k}y_{k-1} - \ldots - a_{n,k}y_{k-n} + b_k u_{k-\tau} \quad (2)$$

Numerous articles have described an approach for the identification of such models; and have illustrated their application to a wide range of practical examples: see e.g. [13] [19] and the references therein. Note that (2) represents a subset of the entire class of SDP models. Nonetheless, it encompass a wide range of nonlinear structures and has recently proven useful for the control of hydraulically operated mobile robots, as used by the construction and nuclear industries [18].

Previous articles [12] have also considered the SDP–NMSS representation of equation (2):

$$\mathbf{x}_{k+1} = \mathbf{F}_k\mathbf{x}_k + \mathbf{g}_k u_k + \mathbf{d}r_{k+1} \;\; ; \;\; y_k = \mathbf{h}\mathbf{x}_k \quad (3)$$

where the $n+\tau$ dimensional state vector is:

$$\mathbf{x}_k = \begin{bmatrix} y_k & \cdots & y_{k-n+1} & u_{k-1} & \cdots & u_{k-\tau+1} & z_k \end{bmatrix}^T \quad (4)$$

and $z_k = z_{k-1} + [r_k - y_k]$ is the integral–of–error between the reference or command input r_k and the sampled output y_k. As usual for NMSS design, inherent type 1 servomechanism performance is introduced by means of this integral–of–error state [14]. The time invariant command $\mathbf{d}$ and observation $\mathbf{h}$ vectors are,

$$\mathbf{d} = \begin{bmatrix} 0 & 0 & \ldots & 0 & 1 \end{bmatrix}^T \;\; ; \;\; \mathbf{h} = \begin{bmatrix} 1 & 0 & \ldots & 0 \end{bmatrix} \quad (5)$$

For $\tau > 1$, the state transition matrix $\mathbf{F}_k$ and input vector $\mathbf{g}_k = \mathbf{g}$ are defined as follows,

$$\begin{aligned} \mathbf{F}_k &= \begin{bmatrix} \mathbf{F}_{1,k} | \mathbf{F}_{2,k} | \mathbf{d} \end{bmatrix} \\ \mathbf{g} &= \begin{bmatrix} 0 & 0 & \cdots & 0 & 1 & 0 & \cdots & 0 & 0 \end{bmatrix}^T \end{aligned} \quad (6)$$

where the $(n+1)$th row element of $\mathbf{g}_k$ is unity, $\mathbf{F}_{1,k} =$

$$\begin{bmatrix} -a_{1,k+1} & \cdots & -a_{n-1,k+1} & -a_{n,k+1} \\ 1 & \cdots & 0 & 0 \\ 0 & \cdots & 0 & 0 \\ \vdots & \ddots & \vdots & \vdots \\ 0 & \cdots & 1 & 0 \\ 0 & \cdots & 0 & 0 \\ 0 & \cdots & 0 & 0 \\ \vdots & \ddots & \vdots & \vdots \\ 0 & \cdots & 0 & 0 \\ a_{1,k+1} & \cdots & a_{n-1,k+1} & a_{n,k+1} \end{bmatrix}$$

and,

$$\mathbf{F}_{2,k} = \begin{bmatrix} 0 & \cdots & 0 & b_{k+1} \\ 0 & \cdots & 0 & 0 \\ 0 & \cdots & 0 & 0 \\ \vdots & \ddots & \vdots & \vdots \\ 0 & \cdots & 0 & 0 \\ 0 & \cdots & 0 & 0 \\ 1 & \cdots & 0 & 0 \\ \vdots & \ddots & \vdots & \vdots \\ 0 & \cdots & 1 & 0 \\ 0 & \cdots & 0 & -b_{k+1} \end{bmatrix}$$

Note that $\mathbf{F}_{2,k}$ has dimension $(n+\tau)\times(\tau-1)$, while the $(n+1)$th row of $\mathbf{F}_k$ consists entirely of zeros. Finally, in the case that $\tau=1$, the state transition matrix is reduced to $\mathbf{F}_k=[\mathbf{F}_{1,k}|\mathbf{d}]$ and the input vector becomes,

$$\mathbf{g}_k=\begin{bmatrix} b_{1,k+1} & 0 & \cdots 0 & -b_{1,k+1}\end{bmatrix}^T$$

The quasi–linear structure of the SDP–NMSS model means that, at each sampling instant, it can be considered as a 'frozen' linear system. This formulation is then used to design a state variable feedback control law,

$$u_k=-\mathbf{c}_k\mathbf{x}_k \tag{7}$$

where,

$$\mathbf{c}_k=\begin{bmatrix} f_{0,k} & \ldots & f_{n-1,k} & g_{1,k} & \ldots & g_{\tau-1,k} & -k_{I,k}\end{bmatrix} \tag{8}$$

is the state dependent control gain vector. Applying the control algorithm (7) to the open–loop NMSS model (3), yields the closed–loop control system,

$$\mathbf{x}_{k+1}=\mathbf{A}_k\mathbf{x}_k+\mathbf{d}r_{k+1}\ \ ;\ \ y_k=\mathbf{h}\mathbf{x}_k \tag{9}$$

where $\mathbf{A}_k=(\mathbf{F}_k-\mathbf{g}_k\mathbf{c}_k)$. The following section derives an algorithm for determining $\mathbf{c}_k$ such that, for an externally specified command r_k, equations (9) yield a closed–loop output response y_k equal to that chosen by the designer.

III. Nonlinear Pole Assignment

To develop a nonlinear pole assignment algorithm, define a $n+\tau$ square matrix $\mathbf{D}$ with user specified (arbitrary) eigenvalues p_i $(i=1,\ldots,n+\tau)$. To satisfy formating constraints, $\mathbf{D}$ is shown in Fig. 2 and Fig. 3 for the cases that $\tau=1$ and $\tau>1$ respectively. In both cases, the eigenvalues of $\mathbf{D}$ are equivalent to the roots of the desired closed–loop characteristic polynomial,

$$D(z^{-1})=1+d_1z^{-1}+\ldots+d_{n+\tau}z^{-(n+\tau)} \tag{10}$$

where d_i are design coefficients and z^{-1} is the backward shift operator, i.e. $z^{-i}y_k=y_{k-i}$.

A. SDP–NMSS Pole Assignment with $\tau=1$

With $\tau=1$ the nonlinear pole assignment solution follows directly from an analogy with linear systems, here by equating either the top or bottom row of $\mathbf{D}$ in Fig. 2 with $\mathbf{A}_k=(\mathbf{F}_k-\mathbf{g}_k\mathbf{c}_k)$ at each sampling instant k. This approach yields an equivalent solution to that obtained in the linear case [14], albeit here with the control gains expressed as state dependent functions of time $a_{1,k+1}\cdots a_{n,k+1}$ and b_{k+1}.

Proposition 1 Assuming no model mismatch and $\tau=1$, the SDP control algorithm (7), where $\mathbf{c}_k$ is obtained as stated above, applied to the nonlinear model (2) or its equivalent (3), yields the following output response: $y_k=(1+d_1+\ldots+d_{n+1})\,r_{k-1}/D(z^{-1})$, i.e. the same solution as for linear pole assignment. With stable design poles, closed–loop stability clearly follows.

Demonstration Under these conditions, it is straightforward to show that the closed–loop state transition matrix $\mathbf{A}_k$ in (9) is time invariant and equal to $\mathbf{D}$ $\forall k$.

B. SDP–NMSS Pole Assignment with $\tau>1$

With $\tau>1$, a transformation of the state vector (4) is required, i.e. $\bar{\mathbf{x}}_k=\mathbf{T}_k\mathbf{x}_k$ where $\mathbf{T}_k$ is the $n+\tau$ square matrix defined in Fig. 4. The transformed open–loop model is,

$$\mathbf{T}_{k+1}\mathbf{x}_{k+1}=\mathbf{F}_k\mathbf{T}_k\mathbf{x}_k+\mathbf{g}u_k+\mathbf{d}r_{k+1}\ ;\ y_k=\mathbf{h}\mathbf{T}_k\mathbf{x}_k$$

Substituting from equation (7) and rearranging yields,

$$\mathbf{x}_{k+1}=\mathbf{T}_{k+1}^{-1}\left(\mathbf{F}_k-\mathbf{g}\mathbf{c}_k\right)\mathbf{T}_k\mathbf{x}_k+\mathbf{T}_{k+1}^{-1}\mathbf{d}r_{k+1} \tag{11}$$

Equating the closed–loop state transition matrix above with the desired matrix $\mathbf{D}$ in Fig. 3, and re–arranging yields,

$$\mathbf{T}_{k+1}^{-1}\mathbf{F}_k\mathbf{T}_k-\mathbf{D}=\mathbf{T}_{k+1}^{-1}\mathbf{g}\mathbf{c}_k\mathbf{T}_k \tag{12}$$

With the particular transformation chosen here, the first n and last $\tau-1$ rows of both $\mathbf{T}_{k+1}^{-1}\mathbf{F}_k\mathbf{T}_k-\mathbf{D}$ and $\mathbf{T}_{k+1}^{-1}\mathbf{g}\mathbf{c}_k\mathbf{T}_k$ consist only of zeros. By equating the $(n+1)$th row of equation (12), and solving the resultant set of $n+\tau$ simultaneous equations, suitable control gains (8) are obtained.

This approach yields the same control gains as those quoted in another recent article by the authors [12]. However, the latter utilises an algebraic approach. By contrast, the present discussion has obtained the control gains directly from the NMSS model, which better lends itself to controllability and stability analysis, as shown below.

Proposition 2 Assuming no model mismatch and $\tau>1$, the SDP control algorithm (7), where $\mathbf{c}_k$ is obtained using equation (12), applied to the nonlinear model (2) or its equivalent (3), yields the following output response: $y_k=(1+d_1+\ldots+d_{n+\tau})\,r_{k-\tau}/D(z^{-1})$, i.e. the same solution as for linear pole assignment. With stable design poles, closed–loop stability clearly follows.

Demonstration When the SDP–NMSS control gains are determined as described above, the closed–loop transition matrix in (9), can always be decomposed into $\mathbf{A}_k=(\mathbf{F}_k-\mathbf{g}_k\mathbf{c}_k)=\mathbf{T}_{k+1}\mathbf{D}\mathbf{T}_k^{-1}$. Hence, pre–multiplying the state equations in (9) by $\mathbf{T}_{k+1}^{-1}$ yields,

$$\tilde{\mathbf{x}}_{k+1}=\mathbf{D}\tilde{\mathbf{x}}_k+\mathbf{T}_{k+1}^{-1}\mathbf{d}r_{k+1}\ \ ;\ \ y_k=\mathbf{h}\tilde{\mathbf{x}}_k \tag{13}$$

where $\tilde{\mathbf{x}}_k=\mathbf{T}_k^{-1}\mathbf{x}_k$. The closed–loop transition matrix is now in a linear time invariant form $\mathbf{D}$, albeit for a transformed state vector $\tilde{\mathbf{x}}_k$. Successive substitutions using (13) yields,

$$\tilde{\mathbf{x}}_k=\mathbf{D}^{n+\tau}\tilde{\mathbf{x}}_{k-n-\tau}+\mathbf{D}^{n+\tau-1}\mathbf{d}r_{k-n-\tau+1}+\ldots+\mathbf{D}^0\mathbf{d}r_k$$

Note from the characteristic polynomial (10) and the Cayley-Hamilton theorem that $\mathbf{D}^{n+\tau}+d_1\mathbf{D}^{n+\tau-1}+\ldots+d_{n+\tau-1}\mathbf{D}+d_{n+\tau}\mathbf{I}=\mathbf{0}$, i.e. a matrix of zeros. Hence, taking $\tilde{\mathbf{x}}_k+d_1\tilde{\mathbf{x}}_{k-1}+\ldots+d_{n+\tau}\tilde{\mathbf{x}}_{k-n-\tau}$ and re-arranging yields,

$$\begin{aligned}\tilde{\mathbf{x}}_k &= -d_1\tilde{\mathbf{x}}_{k-1}-d_2\tilde{\mathbf{x}}_{k-2}-\ldots-d_{n+\tau}\tilde{\mathbf{x}}_{k-n-\tau}\\ &+ \left(\mathbf{D}^{n+\tau-1}+d_1\mathbf{D}^{n+\tau-2}+\ldots+d_{n+\tau-1}\mathbf{I}\right)\mathbf{d}r_{k-n-\tau+1}\\ &+ \ldots+\left(\mathbf{D}+d_1\mathbf{I}\right)\mathbf{d}r_{k-1}+\mathbf{d}r_k\end{aligned} \tag{14}$$

from which the time response of each state can be determined for given r_k. Furthermore, since the observation equation is $y_k=\mathbf{h}\tilde{\mathbf{x}}_k=\mathbf{h}\mathbf{T}_k^{-1}\mathbf{x}_k=\mathbf{h}\mathbf{x}_k$, the transformation does not affect the first element of the state vector and it is a trivial

$$\mathbf{D} = \begin{bmatrix} d_2 + \cdots + d_{n+1} & d_3 + \cdots + d_{n+1} & \cdots & d_{n+1} & 1 + d_1 + d_2 + \cdots + d_{n+1} \\ 1 & 0 & \cdots & 0 & 0 \\ 0 & 1 & \cdots & 0 & 0 \\ \vdots & \vdots & \ddots & \vdots & \vdots \\ -d_2 - \cdots - d_{n+1} & -d_3 - \cdots - d_{n+1} & \cdots & -d_{n+1} & -1 - d_1 - d_2 - \cdots - d_{n+1} \end{bmatrix}$$

Fig. 2. Design matrix based on the polynomial (10) for SDP–NMSS nonlinear pole assignment with $\tau = 1$.

$$\begin{bmatrix} 0 & 0 & \cdots & 0 & 0 & \cdots & 1 & 0 \\ 1 & 0 & \cdots & 0 & 0 & \cdots & 0 & 0 \\ 0 & 1 & \cdots & 0 & 0 & \cdots & 0 & 0 \\ \vdots & \vdots & \ddots & \vdots & \vdots & \ddots & \vdots & \vdots \\ d_{n+\tau} + \cdots + d_{n+1}, & d_{n+\tau} + \cdots + d_{n+2}, & \cdots & d_{n+\tau} & -1 - d_1 & \cdots & -1 - d_1 - \cdots - d_{\tau-1}, & 1 + d_1 + \cdots + d_{n+\tau} \\ 0 & 0 & \cdots & 0 & 1 & \cdots & 0 & 0 \\ \vdots & \vdots & \ddots & \vdots & \vdots & \ddots & \vdots & \vdots \\ 0 & 0 & \cdots & 0 & 0 & \cdots & -1 & 1 \end{bmatrix}$$

Fig. 3. Design matrix $\mathbf{D}$ based on the polynomial (10) for SDP–NMSS nonlinear pole assignment with $\tau > 1$.

$$\begin{bmatrix} 1 & 0 & \cdots & 0 & \cdots & 0 & 0 & 0 \\ 0 & 1 & \cdots & 0 & \cdots & 0 & 0 & 0 \\ \vdots & \vdots & & \vdots & & \vdots & \vdots & \vdots \\ 0 & 0 & \cdots & 1 & \cdots & 0 & 0 & 0 \\ -a_{\tau-1,k+1} + \cdots & -a_{\tau,k+1} + \cdots & \cdots & -a_{n+\tau-2,k} + \cdots & \cdots & & & \\ \vdots & \vdots & & \vdots & & \vdots & \vdots & \vdots \\ -a_{2,k+1} + a_{1,k}a_{1,k+1} & -a_{3,k+1} + a_{2,k}a_{1,k+1} & \cdots & -a_{n+1,k} + a_{n,k}a_{1,k+1} & \cdots & b_{k+1} & -b_k a_{1,k+1} & 0 \\ -a_{1,k} & -a_{2,k} & \cdots & -a_{n,k} & \cdots & -a_{n+\tau-2,k} & b_k & 0 \\ 0 & 0 & \cdots & 0 & \cdots & 0 & 0 & 1 \end{bmatrix}$$

Fig. 4. Transformation matrix $\mathbf{T}_{k-1}^{-1}$ for SDP–NMSS nonlinear pole assignment (inverse at sample $k-1$ shown for brevity; $a_{i,k} = 0$ for $i > n$).

matter to obtain the output response from equation (14). In this regard, note that $\mathbf{hId} = 0$, $\mathbf{hAd} = 0$ (etc.) and $\mathbf{hA}^{n+\tau-1}\mathbf{d} = 1 + d_1 + \ldots + d_{n+\tau}$, hence, $y_k = -d_1 y_{k-1} - d_2 y_{k-2} - \ldots - d_{n+\tau} y_{k-n-\tau} + (1 + d_1 + \ldots + d_{n+\tau})\, r_{k-\tau}$. Expressed as a discrete–time Transfer Function in z^{-1}, this has the desired characteristic polynomial (10), time invariant scalar numerator and a time delay of τ samples, as required.

C. Controllability

Substitution [20] using the open–loop SDP–NMSS state equation (3), yields the following controllability matrix for the $\tau > 1$ case at sample k,

$$\mathbf{S}_k = \begin{bmatrix} \mathbf{g}, & \mathbf{F}_{k+n+\tau-2}\mathbf{g}, & \ldots, & \mathbf{F}_{k+n+\tau-2} \ldots \mathbf{F}_k \mathbf{g} \end{bmatrix} \quad (15)$$

which is non–singular if and only if $b_k \neq 0, \forall k$. This result is equivalent to the pole assignability proposition developed by [12]. Examination of the time indices in $\mathbf{T}_k$ shows that the algorithm requires a forward shift of the parameters. In this regard, it is important to recall their state dependent form. For many engineering devices, these parameters are functions of the *delayed* input and output signals, hence a forward shift does not usually cause problems.

IV. Simulation Example

Preliminary open–loop step experiments on the Hydro–Lek manipulator suggest that a first order linear difference equation, i.e. $y_k = -a_1 y_{k-1} + b u_{k-\tau}$, provides an approximate representation of individual joints, with the time delay τ depending on the chosen joint and sampling interval. Here, y_k is the joint angle and u_k is the scaled voltage in the range ± 1000, while $\{a_1, b\}$ are time invariant parameters.

Further analysis of open–loop data collected from the Hydro–Lek HLK–7W, reveals limitations in the linear model. In particular, the value of b depends on the presently applied voltage to the system. In these cases, SDP analysis suggests that a more appropriate model for individual joints is (2) with $n = 1$,

$$y_k = -a_k y_{k-1} + b_k u_{k-\tau} \quad (16)$$

where (for brevity) $a_{k,1}$ is denoted a_k. Preliminary SDP analysis of open–loop data from one particular joint, sampled at 16Hz, suggests $\tau = 3$. In the following discussion, this model is used as a worked example to illustrate the control approach. The SDP–NMSS model (3) is defined by

$\mathbf{x}_k = \begin{bmatrix} y_k & u_{k-1} & u_{k-2} & z_k \end{bmatrix}^T$, $\mathbf{g} = \begin{bmatrix} 0 & 1 & 0 & 0 \end{bmatrix}^T$ and,

$$\mathbf{F}_k = \begin{bmatrix} -a_{k+1} & 0 & b_{k+1} & 0 \\ 0 & 0 & 0 & 0 \\ 0 & 1 & 0 & 0 \\ a_{k+1} & 0 & -b_{k+1} & 1 \end{bmatrix} \tag{17}$$

The transformation matrix (based on Fig. 4) is,

$$\mathbf{T}_k = \begin{bmatrix} 1 & 0 & 0 & 0 \\ 0 & \frac{1}{b_{k+2}} & \frac{a_{k+2}}{b_{k+2}} & 0 \\ \frac{a_{k+1}}{b_{k+1}} & 0 & \frac{1}{b_{k+1}} & 0 \\ 0 & 0 & 0 & 1 \end{bmatrix}; \tag{18}$$

The design transition matrix (Fig. 3) is,

$$\mathbf{D} = \begin{bmatrix} 0 & 0 & 1 & 0 \\ d_4 & -1-d_1 & -1-d_1-d_2 & \tilde{d} \\ 0 & 1 & 0 & 0 \\ 0 & 0 & -1 & 1 \end{bmatrix} \tag{19}$$

where $\tilde{d} = 1 + d_1 + d_2 + d_3 + d_4$. Substituting these into (12) and equating yields,

$$\begin{aligned} f_{0,k} &= \frac{-a_{k+1}\left(1 + d_1 + d_2 - a_{k+2}\left(1 + d_1 - a_{k+3}\right)\right) - d_4}{b_{k+3}} \\ g_{1,k} &= \frac{b_{k+2}\left(1 + d_1 - a_{k+3}\right)}{b_{k+3}} \\ g_{2,k} &= \frac{b_{k+1}\left(1 + d_1 + d_2 - a_{k+2}\right)}{b_{k+3}} \\ k_{I,k} &= \frac{1 + d_1 + d_2 + d_3 + d_4}{b_{k+3}} \end{aligned} \tag{20}$$

The closed–loop transition matrix in equations (9) can be written as $\mathbf{A}_{k+1} = \mathbf{T}_{k+1}\mathbf{D}\mathbf{T}_k^{-1}$, where $\mathbf{T}_k$ and $\mathbf{D}$ are defined by (18) and (19) respectively. Hence, using Proposition 1, the closed–loop response is defined by the following linear Transfer Function,

$$y_k = \frac{1 + d_1 + d_2 + d_3 + d_4}{1 + d_1 z^{-1} + d_2 z^{-2} + d_3 z^{-3} + d_4 z^{-4}} r_k \tag{21}$$

In other words, the nonlinear terms are eliminated in the closed–loop and so the nature of the state dependency does not influence the theoretical response.

To illustrate, Fig. 5 shows the response of the closed–loop system based on $d_1 = d_2 = d_3 = d_4 = 0$ and using arbitrarily defined state dependencies for a_k and b_k. Following various step changes in the command at sample k, the SDP controller (20) yields the expected deadbeat output response. Of course, this is an unrealistic simulation example and deadbeat design would not be used in practice. It was chosen to illustrate the stability of the solution, even in this extreme case. Naturally all the results above assume zero model mismatch, the same assumption as for linear pole assignment design. The robustness to model mismatch and disturbances is the subject of current research by the authors. However, simulation and experimental results support the practical utility of the approach [12]. The authors are presently developing control systems for the Brokk Hydro–Lek system using this new pole assignment approach, and will report on the experimental results in future publications. In this regard, the recently developed hardware arrangements are summarised below.

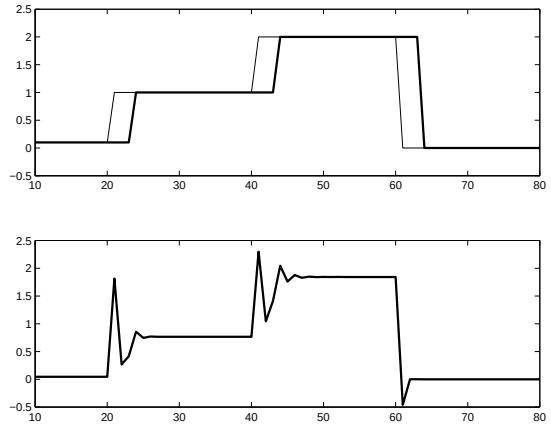

Fig. 5. Deadbeat simulation example. Top subplot: command input (thin trace) and closed–loop response of the nonlinear model (16) with $\tau = 3$. Lower subplot: control input. All these variables are plotted against sample number.

V. Hardware Framework

The hardware configuration consists of two human arm–like off–the–shelf manipulators, whose joints are controlled using potentiometer sensors and hydraulic actuators; and a mobile platform to support and transport the multi–arm robot system (Fig. 1). The movements of the manipulator joints are controlled through the integration of the hardware and software using National Instrument (NI) tools. Full details of these arrangements are given by [3] and [4].

The Brokk 40 base machine [21] consists of a moving vehicle with a single 5–Degree–of–Freedom (DOF) manipulator and five linear actuators; a hydraulic tank; a controller and a remote control device designed to operate the vehicle and its manipulator. The Brokk 40 is the smallest robot in the Brokk family and is an off–the–shelf machine which was designed for heavy demolition tasks and to pass through narrow spaces such as 650mm wide doorways. It is electrically powered to facilitate internal use.

The Hydro–Lek HLK–7W [22] is a 6–degree–of-freedom manipulator with a continuous jaw rotation mechanism and dual function gripper fitted with a pressure sensor. The gripper is designed to grip an object and also to cut ropes up to 19mm diameter. The azimuth yaw, shoulder pitch, elbow pitch, forearm roll and wrist pitch joints are fitted with potentiometer feedback sensors. The mounting bracket is designed to hold the weight of the two arms with full payloads. The other side of the bracket is designed to be fitted to the end of the Brokk machine manipulator where it can be rotated forward and backwards. The system provides a stable platform for the attached tools. Locking facilities such

as non–return valves or self–locking actuators can be used to lock the manipulator joints at any position and orientation even when the robot is de–powered.

To illustrate the feasibility of the SDP approach, equation (16) is fitted to preliminary data collected from one Hydro–Lek HLK–7W joint. In this case, b_k has a clear relationship with the delayed input signal, as illustrated in Fig. 6, in which parameter estimates (circles) and a polynominal fit are shown. Note that the deadband of the device ensures no arm movement until the voltage exceeds 1.2 (scaled units) in Fig. 6, hence the $b_k \neq 0$ requirement discussed in section III-C is not a problem. Also, the results in Fig. 6 are based on an initial linear analysis of the step response data, rather than the SDP identification approach discussed above. Nonetheless, these preliminary results pressage the likely utility of the SDP modelling approach. Detailed SDP analysis, model evaluation and control implementation are the subject of current research by the authors.

VI. Conclusions

The Brokk Hydro–Lek configuration is a good example of a robotic system that can be designed for hazardous nuclear decommissioning applications. It demonstrates the complexity of such a system from a number of aspects, such as the need for mobility, control, sensors, system design, integration and interfacing using modern tools that are available off–the–shelf. However, under automatic control, the manipulator can sometimes suffer from a relatively slow and imprecise control action because of limitations in existing linear feedback algorithms.

This paper has developed a pole assignment algorithm for the control of nonlinear dynamic systems described by State Dependent Parameter (SDP) models. The state variable feedback control algorithm is derived from a non–minimal state space model, necessitating the introduction of a state dependent transformation matrix. The new approach yields equivalent control gains to those already presented (without derivation) by [12]. However, the state space derivation here, lends itself to a more concise and transparent description of the closed–loop behaviour. In this regard, the paper shows that the closed–loop system reduces to a linear transfer function with the specified stable (design) poles.

Control gains are determined for a worked example, based on preliminary modelling results for an illustrative robot arm joint. However, the present paper concentrates on a presentation of the new control methodology, hence is limited to a simplistic simulation example. Clearly the next stage of the research is to develop practical control systems for each joint using the new pole assignment approach and to evaluate these for the full Brokk Hydro–Lek system.

VII. Acknowledgements

The authors are grateful for the support of the UK Nuclear Decommissioning Authority (NDA).

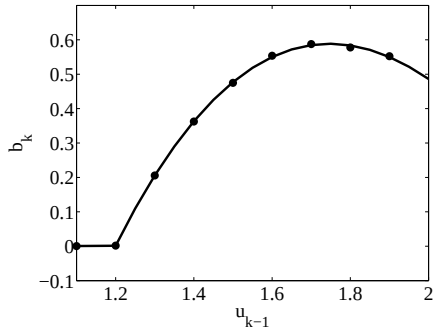

Fig. 6. State dependent parameter b_k plotted against state variable u_{k-1} based on experimental data collected from one Hydro–Lek joint.

References

[1] NDA www.nda.gov.uk (accessed 2007)
[2] D. W. Seward, C. M. Pace, and R. Agate. Safe and effective navigation of autonomous robots in hazardous environments. *Journal of Autonomous Robots*, 22:223–242, 1999.
[3] M.J. Bakari, K.M. Zeid, and D.W. Seward. Development of a multi-arm mobile robot for nuclear decommissioning tasks. *International Journal of Advanced Robotic Systems*, 4:387–406, 2007.
[4] M. J. Bakari, D. W. Seward, and C. J. Taylor. The development of a prototype of a multi–arm robotic system ... nuclear industry In *12th International Conference on Environmental Remediation and Radioactive Waste Management*, Liverpool, UK, October 2009.
[5] Q. Ha, D. Rye, and H. Durrant-Whyte. Fuzzy moving sliding mode control ... robotic manipulators. *Automatica*, 35:607–616, 1999.
[6] M.-H. Chiang and H. Murrenhoff. *Adaptive servo-control for hydraulic excavators*. Professional Engineering Publishing Limited, UK, 1998.
[7] B. Fidan, Y. Zhang, and P. A. Ioannou. Adaptive control of a class of slowly time varying systems with modeling uncertainties. *IEEE Transactions on Automatic Control*, 50:915–920, 2005.
[8] T. Cimen. State–dependent Riccati equation SDRE control: a survey. In *IFAC World Congress*, Seoul, Korea, 2008.
[9] M. W. Wonham. On pole assignment in multi–input controllable linear systems. *IEEE Transactions Automatic Control*, 12:660–665, 1967.
[10] A. Isidori. *Nonlinear control systems*. Springer–Verlag, 1995.
[11] N. Kazantzis and C. Kravaris. Synthesis of state feedback regulators for nonlinear processes. *Chemical Eng. Science*, 55:3437–3449, 2000.
[12] C. J. Taylor, A. Chotai, and P. C. Young. Nonlinear control by input–output state variable feedback pole assignment. *International Journal of Control*, 82:1029–1044, 2009.
[13] P. C. Young, P. McKenna, and J. Bruun. Identification of nonlinear stochastic systems by state dependent parameter estimation. *International Journal of Control*, 74:1837–1857, 2001.
[14] P. C. Young, M. A. Behzadi, C. L. Wang, and A. Chotai. Direct digital and adaptive control by input–output, state variable feedback pole assignment. *International Journal of Control*, 46:1867–1881, 1987.
[15] C. J. Taylor, A. Chotai, and P. C. Young. State space control system design based on non–minimal state–variable feedback. *International Journal of Control*, 73:1329–1345, 2000.
[16] J. Gu, C. J. Taylor, and D. W. Seward. The automation of bucket position for the intelligent excavator LUCIE using the PIP control strategy. *Journal of Computer-Aided Civil and Infrastructure Engineering*, 12:16–27, 2004.
[17] E. M. Shaban, S. Ako, C. J. Taylor, and D. W. Seward. Development of an automated verticality alignment system for a vibro-lance. *Automation in Construction*, 17:645–655, 2008.
[18] C. J. Taylor, E. M. Shaban, M. A. Stables, and S. Ako. Proportional–Integral–Plus (PIP) control applications of state dependent parameter models. *IMECHE Proceedings Part I*, 221(17):1019–1032, 2007.
[19] C. J. Taylor, D. J. Pedregal, P. C. Young, and W. Tych. Environmental time series analysis and forecasting with the Captain Toolbox. *Environmental Modelling and Software*, 22(6):797–814, 2007.
[20] B. C. Kuo. *Digital Control Systems*. CBS Publishing Tokyo, 1980.
[21] Brokk UK Ltd. www.brokk.com
[22] Hydro–Lek Ltd. www.hydro-lek.com